

Vortex-glass transition in superconducting Nb/Cu superlattices

J.E. Villegas and J.L. Vicent

Dpto. Física de Materiales, Universidad Complutense de Madrid, 28040 Madrid, Spain

Abstract

Nb/Cu superconducting superlattices have been fabricated by dc magnetron sputtering. This system shows a vortex glass transition with critical exponents similar to high temperatures superconductors exponents. The transition dymensionality is governed by the superconducting coupling regime. The vortex glass transition shows a *pure* two dimensional behavior in decoupled superlattices and a *quasi*-two dimensional behavior in the superlattice coupling regime.

Since the discovery of High-Tc Superconductors (HTCS) vortex matter Physics has called the attention of researchers in many fields, for example the vortex state provides a perfect realm to study properties of liquid, crystalline and glassy phases. A plethora of different phases is observed in HTCS,¹ induced by the interplay of vortex-vortex interaction, thermal fluctuations, different kinds of disorder, anisotropy, dimensional effects, etc.² But the most remarkable characteristic of the phase diagram is the existence of two different states: a magnetically irreversible zero-resistance state, and a reversible state with dissipative transport properties. In the absence of disorder, the former corresponds to a vortex-solid phase with topological order, and the latter to a vortex-liquid phase, both of them separated by a first-order melting transition. In the presence of strong quenched disorder, however, the topological order of the vortex-lattice is lost, and the zero-resistance state corresponds to a vortex-glass (VG), and the transition into the dissipative liquid state becomes a continuous second-order phase transition.^{3,4}

After the rich phenomenology of vortex-phases came out with HTSC, Low-Tc Superconductors (LTCS) have been seldom revisited to check the possible application of HTCS paradigms. The existence of a melting transition in Nb single crystals has been reported,^{5–7} but in the case of Nb thin films the existence of a glass transition remains controversial.^{8,9}

In this paper, we report on the observation of VG transitions in sputtered Nb/Cu low-temperature superconducting superlattices. This system has been chosen mainly because the presence of quenched disorder is similar to the one existing in sputtered Nb thin films and because the artificially layered structure allows tailoring the anisotropy of the system in a controllable fashion. In particular, the coupling of Nb layers through the Cu spacer can be easily tuned.¹⁰ This has allowed us studying the dimensionality of the VG transition in several different coupling regimes.

The VG transition has been investigated by measuring the electrical transport properties in the mixed state of superlattices, in particular isothermal I-V characteristics in applied magnetic fields. These characteristics have been collapsed, according to the scaling rules proposed in the VG theory, in terms of critical exponents.⁴ Besides, the consistency of the scaling analysis has been checked with some independent criterion, as recently proposed.¹¹ Moreover, we have found a dimensional crossover for a *quasi*-2D into a *pure* 2D VG transition, governed by the coupling of Nb layers in the superlattice.

Nb/Cu superlattices were grown on Si (100) substrates using *dc* magnetron sputtering at

room temperature in Ar atmosphere. Several series of superlattices $\text{Cu}_d[\text{Nb}_{d'}/\text{Cu}_d]_N$ were grown with N being the number of bilayers. Structural characterization was made by X-Ray diffraction (XRD). The structural properties of Nb/Cu superlattices have been investigated early by other authors.¹² In our multilayers XRD shows that Cu layers are oriented (111), while Nb ones are (110). We have refined the spectra using SUPREX program.¹³ From refinements the modulation length Λ , as well as several sources of disorder at the interfaces, like roughness or interdiffusion have been obtained. The samples studied here did not present interdiffusion, and have moderate roughness at the interfaces, ranging from 0.2 to 0.6 nm, being larger when the Nb layers are thicker. The samples were lithographed by wet etching into a measuring bridge 1 mm long and 100 μm wide for magnetotransport experiments with standard four-probe configuration.

Magnetotransport experiments were made in a liquid He cryostat provided with a superconducting solenoid. The superconducting coherence length ξ_S as a function of temperature was calculated from measured upper critical fields $H_{c2}(T)$, obtained from magnetoresistance measurements at constant fixed temperatures $R(H)_T$. The in-plane coherence length $\xi_{S\parallel}$ (parallel to Nb/Cu interfaces) and the perpendicular one $\xi_{S\perp}$ have been calculated by using $\xi_{S\parallel}(T) = [\phi_0/2\pi H_{c2\perp}(T)]^{1/2}$ and $\xi_{S\perp}(T) = \left[\phi_0 H_{c2\perp}(T) / 2\pi (H_{c2\parallel}(T))^2\right]^{1/2}$ respectively.¹⁰ As an example, the observed behavior for sample $\text{Nb}_{13\text{nm}}/\text{Cu}_{27\text{nm}}$ is shown in Fig. 1. The perpendicular critical field displays typical linear dependence on temperature $H_{c2\perp}(T) \propto (1 - T/T_c)$ (see Fig. 1 inset). However, the parallel critical field shows up a crossover from linear dependence $H_{c2\parallel}(T) \propto (1 - T/T_c)$ at high enough temperatures to square-root $H_{c2\parallel}(T) \propto (1 - T/T_c)^{1/2}$ at lower temperatures. A dimensional crossover takes place when the perpendicular coherence length $\xi_{S\perp}(T)$ reaches a value of the order of d_{Cu} (thickness of Cu in the superlattice). Below the crossover temperature, $T_{2D} \approx 0.5T_c$, the Nb layers are decoupled, showing up two-dimensional (2D) behavior.¹⁰ In other cases, as for instance $\text{Nb}_{3.4\text{nm}}/\text{Cu}_{2.4\text{nm}}$, $\xi_{S\perp}(T) > d_{\text{Cu}}$ at all temperatures, and thus superlattices are always in the coupled regime.

We have measured I-V characteristics with magnetic field H applied perpendicular to Nb/Cu layers. For each fixed value of applied field H , we measured a set (~ 20) of isothermal I-V curves at decreasing temperatures, as those shown in Fig. 2 and Fig. 3. For all measured samples and applied magnetic fields the results are similar. The isotherm at the highest temperature displays linear behavior at all current levels, with Ohmic resistance $R = V/I \approx R_n$, at this temperature $H = H_{c2\perp}$. For characteristics at slightly lower temperatures, the

Ohmic response is observed only up to a threshold current level I_{nl} , above which the curves are non-linear. The Ohmic resistance in the low-current limit $\lim_{I \rightarrow 0} V/I \neq 0$ is smaller as the temperature decreases, as well as the onset of non-linear response I_{nl} shifts to lower current levels as temperature is reduced. Below a given temperature, isotherms become highly non-linear within the whole experimental window, and isotherms show up negative curvature in the low-current limit yielding zero resistance $\lim_{I \rightarrow 0} V/I = 0$.

The phenomenology described above suggests the existence of a continuous transition from a truly superconducting phase with zero-resistance (VG) to a vortex-liquid dissipative phase closer to H_{c2} . As proposed by Fisher-Fisher-Huse,⁴ and shown experimentally for many HCTS systems, this glass-transition is a second order transition and the physical quantities must scale with the VG correlation length ξ_{VG} and the characteristic relaxation time τ . These two magnitudes diverge as temperature approaches the glass transition temperature T_g , following $\xi_{VG} \propto (T - T_g)^{-\nu}$ and $\tau \propto (T - T_g)^{-z\nu}$, with z and ν the dynamic and static critical exponents. Scaling laws have been proposed to collapse onto a single master curve all I-V (or $E - J$) isotherms within the critical region, by means of the relation⁴

$$E\xi_{VG}\tau \approx J\xi_{VG}^{D-1}\zeta_{\pm} (J\phi_0\xi_{VG}^{D-1}/k_BT) \text{ [Eq. 1]}$$

where D is the dimensionality of the glass transition, ζ_{\pm} is a universal scaling function above (ζ_+) or below (ζ_-) T_g , ϕ_0 the flux quantum, and k_B the Boltzmann constant. We have applied this scaling analysis to I-V characteristics measured within the experimental window $10^{-8}\text{V} < V < 10^{-4}\text{V}$ and $I < 10^{-3}\text{ A}$. The voltage cut-off is 10^{-4} V , since above this limit all characteristics deviate towards Ohmic behavior. Therefore, the scaling analysis is not longer valid.^{11,14,15} This can be seen in the inset of Fig. 2 (b), where the slopes of isotherms [as plotted in Fig 2 (a)], $d(\log V)/d(\log I)$, are displayed.

For Nb/Cu superlattices whose Nb layers are coupled, the scaling analysis yields very good collapses, as the one shown in Fig. 2 (b). Critical exponents were around $z \approx 4$ and $\nu \approx 1.8$, and the dimensionality was always $D=2$. These parameters are not magnetic field or sample dependent. The values of the critical exponents z and ν are within the range 4-6 predicted by theory.⁴ Moreover, we want to underline that the obtained values are very similar to that observed for *quasi*-2D VG transitions in HTCS.^{16,17} For instance, the same values of the critical exponents were found in $\text{YBa}_2\text{Cu}_3\text{O}_{7-\delta}$ thin films.¹⁷ This fact stresses the universality of the VG transition, earlier suggested.^{17,18}

Recently, Strachan et al.¹¹ have proved that the scaling method used is misleading, even in

the case of universal critical exponents with adequate values were found. They have argued that experimental limitations related to voltage sensitivity floor might allow achieving good collapses with arbitrary values of some of the scaling parameters, as for instance T_g . Thus, Strachan *et al.*¹¹ have proposed that a new criterion to unambiguously determine T_g should be met: isotherms above and below T_g , but with equal $|(T - T_g)/T_g|$, must have opposite concavities at the same applied current level. In our Nb/Cu superlattices this criterion was checked for every set of I-V curves that had been successfully scaled. In the inset of Fig 2 (b), the derivatives $d(\log V)/d(\log I)$ of the I-V isotherms shown in Fig. 2 (b) are plotted. From the scaling procedure we obtained $T_g=3.994$ K for this set of isotherms. As can be seen in that Figure, the isotherms above and below this temperature (marked with an arrow in Fig. 2(d)) met the criterion. At the lowest current levels, upward and downward isotherms are observed at similar distance $|(T - T_g)/T_g|$ below and above T_g . Furthermore the VG transitions theory tells that the isotherm at T_g fulfills the relation $E \propto J^{\alpha+1}$ in the low current limit, where $\alpha = (z + 2 - D)/(D - 1)$.⁴ Therefore, using the values obtained in our scaling, $D=2$ and $z \approx 4$, the expected slope of the critical isotherm would be $\alpha + 1 \approx 5$. Although the critical isotherm is not in the set of measured characteristics, we can give lower and upper limits to its slope from those of the isotherms just above and just below T_g . In the low current limit (Fig. 2 (b) inset), the first isotherm below T_g has a slope larger than ~ 5 , whilst the first one above T_g has a slope smaller than ~ 4.5 . Thus the critical isotherm in between them should have a slope around $\sim 4.5-5$, as expected from the independently obtained scaling parameters.

The behavior of superlattices whose Nb layers were decoupled was investigated too. The inset of Fig. 3 (a) shows I-V characteristics of sample Nb_{13nm}/Cu_{27nm} in applied magnetic field $\mu_0 H=0.4$ T, such that all isotherms, within the critical region, were at temperatures well below $T=T_{2D} \approx 0.5T_c$ (see Fig. 1). Attempts to use the scaling rule (Eq. 1) did not yield collapses as the ones obtained in the coupled regime. In fact, from the derivatives of I-V curves [Fig. 3 (b)], one can observe some features that rule out the scaling of these isotherms according to a *quasi*-2D or 3D VG transition. On one hand, it is not possible determining a finite T_g using the criterion outlined above, since two isotherms of opposite concavities at the same current level can not be found. Besides, as can be seen in Fig. 3 (b), a maximum slope of ~ 9 is displayed by the lowest temperature isotherm among those showing up a decreasing slope in the low current limit (marked with an arrow).

The isotherm at T_g should be above this one, and therefore it should have a slope larger than ~ 9 . As we said before, in a *quasi*-2D or 3D VG transition the slope of the critical isotherm is $\alpha + 1 = (z + 2 - D)/(D - 1) + 1$, which would imply that the critical exponent $z > 8$ for $D=2$, or $z > 17$ if $D=3$. These are very high values of the critical exponents, not supported by theory.⁴ As argued earlier,^{16,17} this strongly suggests that a *quasi*-2D or 3D VG transition has to be dismissed. However, a good scaling of the isotherms is achieved by assuming a different *pure* 2D VG transition, as first proposed by Dekker *et al.*¹⁹, and later found in HTSC systems.^{16,17} In a *pure* 2D VG transition, the glass transition temperature $T_g=0$. Therefore a *pure* 2D VG phase does not exist at any finite temperature, although in-plane correlations (2D) develop, diverging as $\xi_{VG} \propto 1/T^{\nu'}$ when temperature approaches $T_g = 0$. In this transition, the scaling of the isotherms is achieved by plotting $\rho \exp[(T_0/T)^p]$ vs. $J/T^{1+\nu'}$, where $\rho = E/J$ is the resistivity, T_0 is a characteristic temperature, and p and $\nu'=2$ are characteristic exponents of the *pure* 2D VG transition. The exponent p is related to the mechanism of vortex motion: $p \geq 1$ for thermal activation over the relevant energy barriers, whereas $p \approx 0.7$ is expected in the case of quantum tunneling across them.¹⁹ As can be seen in Fig. 3 (a), a good collapse has been obtained with parameters $T_0=300 \pm 20$ K, $p=1.05 \pm 0.02$, and $\nu'=2$.

Finally, in our experimental situation, a layered superconductor with magnetic field applied perpendicular to layers, one may distinguish between the in-plane VG correlation length $\xi_{VG\parallel}$, and the perpendicular one $\xi_{VG\perp}$ (along the vortex line).⁴ The *quasi*-2D character of the glass transition was explained in high T_c superconductors assuming that anisotropy induces limited vortex length, that precludes $\xi_{VG\perp}$ to diverge.^{16,17} Thus, when approaching T_g , only $\xi_{VG\parallel}$ diverges up to the macroscopic size of the sample, whereas $\xi_{VG\perp}$ would remain finite with nearly a constant value. This applies to Nb/Cu superlattices in the coupled regime. Following Yamasaki *et al.*¹⁶ and Zefrioui *et al.*¹⁷ we can estimate an upper limit of $\xi_{VG\perp}$ from I-V characteristics. Isotherms above T_g show up Ohmic behavior at low current level, but they become non-linear above I_{nl} . At this current level, the work done by the Lorentz force to create vortex excitations equals the thermal energy,⁴ $J_{nl}\phi_0\xi_{VG\parallel}\xi_{VG\perp} = k_B T$. We used the isotherm at the highest temperature within the critical region, in particular the one at $T=4.038$ K shown in Fig. 3 (a), for which $J_{nl} \approx 125$ Acm⁻². The in-plane correlation length $\xi_{VG\parallel}$ should be larger than the mean inter-vortex distance $a_0 = (\phi_0/\mu_0 H)^{1/2} \approx 130$ nm for $\mu_0 H = 0.11$ T. In particular we assumed $\xi_{VG\parallel} > 2a_0$, and thus we obtained $\xi_{VG\perp} < 90$ nm.

That is, the correlation length along vortex line is always shorter than sample thickness. However, it may be longer than other relevant characteristic lengths, as the superlattice modulation length $\Lambda=40$ nm and the superconducting coherence length $\xi_{S\perp}(T)\approx 35$ nm. We have estimated the vortex length l in the regime where this superlattice is decoupled, in which we observed a *pure* 2D VG transition, with the work done by Lorentz force $J_{nl}\phi_0\xi_{VG\parallel}l = k_B T$.¹⁹ Taking the isotherm at $T=2.150$ K [Fig. 3 (a)], $J_{nl}\approx 80$ Acm⁻², and $\xi_{VG\parallel}>2a_0=150$ nm for $\mu_0 H = 0.4$ T, we get $l < 30$ nm. Therefore, the vortex length l is shorter than superlattice modulation length $\Lambda=40$ nm, and cannot be much longer than the coherence length at this T , $\xi_{S\perp} \approx 20$ nm. A picture emerges from those estimations, in which coherence length $\xi_{S\perp}$ and sample thickness d are the relevant length scales to which correlation length along vortex line $\xi_{VG\perp}$ has to be compared. The *quasi*-2D character of the glass transition in the coupled regime develops since $\xi_{VG\perp}$, longer than $\xi_{S\perp}$, is shorter than sample thickness d . At lower temperatures, Nb layers are decoupled by Cu ones. Therefore the vortex length l is limited below modulation length Λ . Because of this, the vortex length l and coherence length $\xi_{S\perp}$ are similar. This yields a *pure* 2D VG transition. This is similar to what is observed in highly anisotropic HTCS, for which *pure* 2D VG transitions have been observed when vortex length is limited to superconducting coherence length.^{17,20,21}

In summary, we have shown strong evidence of the VG transition in the mixed state of low-temperature superconducting Nb/Cu superlattices. The HTCS analysis applies directly to this system, and the same universality has been observed, in spite of the very small thermal fluctuations of LTCS in comparison with HTCS. Besides, a dimensional crossover from a *quasi*-2D into a *pure* 2D VG transition has been observed, which is governed by the ratio of the VG correlation length ξ_{VG} to the superconducting coherence length ξ_S .

We acknowledge financial support from Spanish Ministerio de Educación y Ciencia under grants MAT2002-04543 and MAT2002-12385-E, and "Ramón Areces" Foundation. We would like to acknowledge Z. Sefrioui and J. Santamaria for discussions.

REFERENCES

- ¹F. Bouquet *et al.* , Nature **411**, 449 (2001).
- ²G. Blatter *et al.*, Rev. Mod. Phys. **64**, 1125 (1994).
- ³M.P.A. Fisher, Phys. Rev. Lett. **62**, 1415 (1989).
- ⁴D. S. Fisher, M.P.A. Fisher and D.A. Huse, Phys. Rev. B **43** 130 (1991).
- ⁵J.W. Lynn *et al.*, Phys. Rev. Lett. **72**, 3413 (1994).
- ⁶P.L. Gammel *et al.*, Phys. Rev Lett. **80**, 833 (1998).
- ⁷X.S. Ling *et al.*, Phys. Rev. Lett. **86**, 712 (2001)
- ⁸M.F. Schmidt, N.E. Israeloff and A.M. Goldman, Phys. Rev. Lett **70**, 2162 (1993).
- ⁹Y. Ando, H. Kubota and S. Tanaka, Phys. Rev. B. **48**, 7716 (1993).
- ¹⁰C.S.L. Chun, G.-G. Zheng, J.L. Vicent, I. K. Schuller, Phys. Rev. B **29**, 4915 (1984).
- ¹¹D.R. Strachan *et al.*, Phys. Rev. Lett. **87**, 067007 (2001).
- ¹²I.K. Schuller, Phys. Rev. Lett. **44**, 1597 (1980); J.-P. Locquet *et al.*, Phys. Rev. B. **38**, 3572 (1988); J.-P. Locquet *et al.* Phys. Rev. B. **39**, 13338 (1989).
- ¹³E.E. Fullerton *et al.*, Phys. Rev. B **45**, 9292 (1992).
- ¹⁴P. J. M. Wöltgens *et al.*, Phys. Rev. B **52**, 4536 (1995).
- ¹⁵P. Voss-deHaan, G. Jakob, and H. Adrian, Phys. Rev. B **60**, 12 443 (1999).
- ¹⁶H. Yamasaki *et al.*, Phys. Rev. B **50**, 12959 (1994).
- ¹⁷Z. Sefrioui *et al.*, Phys. Rev. B **60**, 15423 (1999); E. M. Gonzalez *et al.*, J. Low Temp. Phys. **117**, 675 (1999).
- ¹⁸K. Moloni *et al.*, Phys. Rev. B **56**, 14784 (1997).
- ¹⁹C. Dekker *et al.*, Phys. Rev. Lett **69**, 2717 (1992).
- ²⁰Hai-hu Wen *et al.*, Phys. Rev. Lett. **80**, 3859 (1998).
- ²¹Z. Sefrioui *et al.*, Europhys. Lett. **49**, 679 (1999).

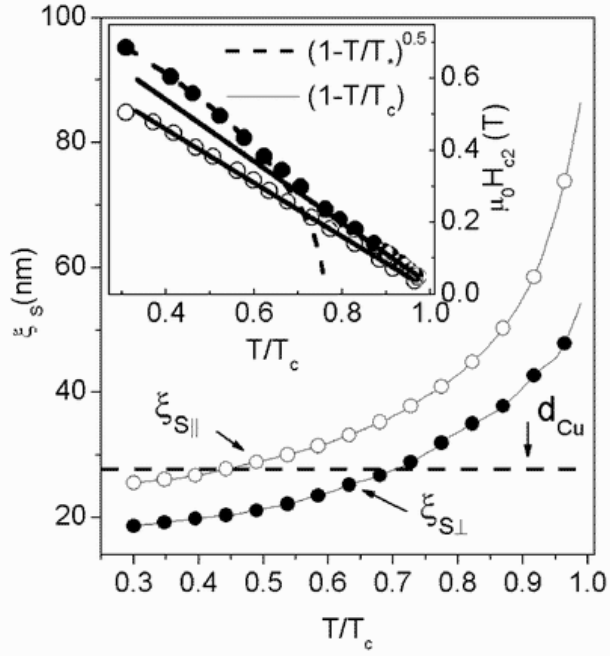


Figure 1
J.E. Villegas et al.

FIG. 1: Superconducting coherence lengths of sample $\text{Cu}_{27\text{nm}}[\text{Nb}_{13\text{nm}}/\text{Cu}_{27\text{nm}}]_{10}$ as a function on temperature, both parallel $\xi_{S||}(T)$ and perpendicular $\xi_{S\perp}(T)$ to Nb/Cu layers. Inset: Measured parallel (black circles) and perpendicular (open circles) critical fields H_{c2} . Solid lines are linear fits $H_{c2\perp}(T) \propto (1-T/T_c)$, while the dashed one is the best fit to $H_{c2||}(T) \propto (1-T/T_c)^{1/2}$.

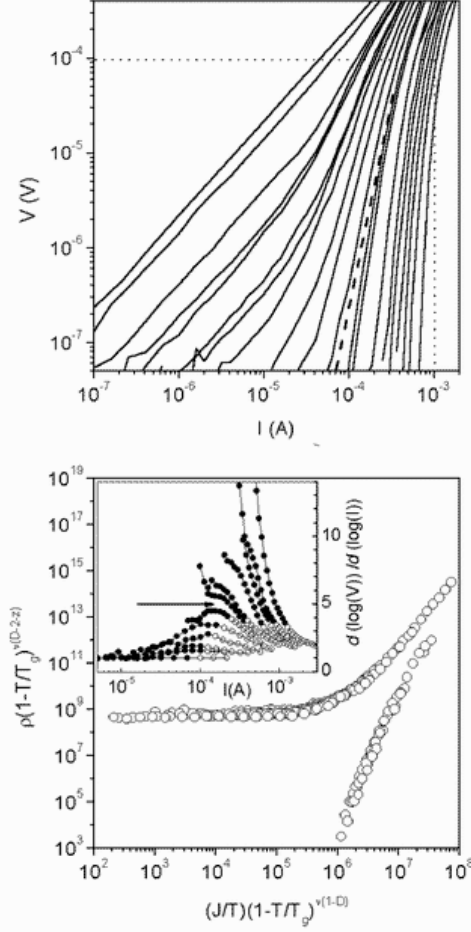


Figure 2
J.E. Villegas et al.

FIG. 2: (a) I-V isotherms for sample $\text{Cu}_{27\text{nm}}[\text{Nb}_{13\text{nm}}/\text{Cu}_{27\text{nm}}]_{10}$ in applied field $\mu_0 H = 0.11$ T at temperatures (from left to right) $4.060 \text{ K} > T > 3.865 \text{ K}$, separated $\sim 5\text{-}15$ mK. The dashed line separates isotherms above and below $T_g = 3.994$ K. Vertical and horizontal dotted lines delimit the experimental window used for scaling. (b) Scaling of the above isotherms as explained in the text. Inset: Derivatives of the $\log(I)$ - $\log(V)$ isotherms at temperatures (from bottom to top) $4.060 \text{ K} > T > 3.908 \text{ K}$. Black dots are within the experimental window used for scaling. The arrow separates derivatives of isotherms just below and above T_g .

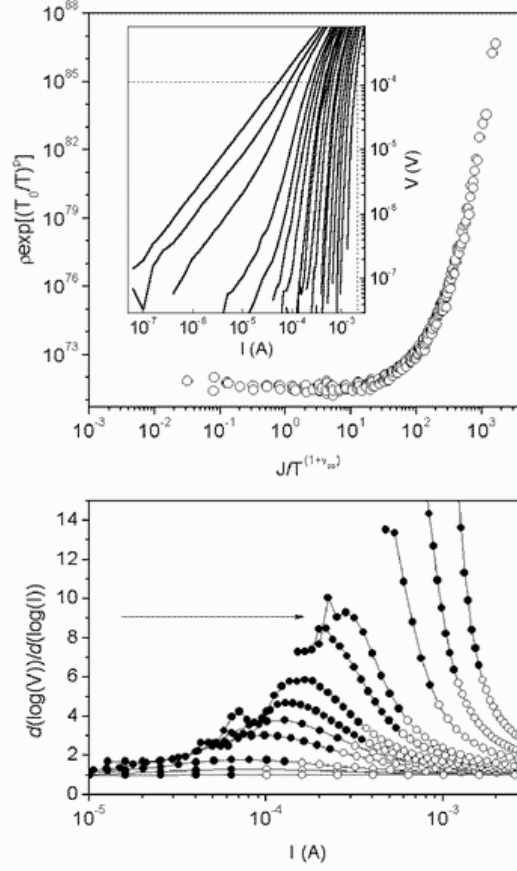


Figure 3
J.E. Villegas et al.

FIG. 3: (a) Scaling of the isotherms shown in the inset with a *pure* 2D VG model. Inset: I-V isotherms for sample $\text{Cu}_{27\text{nm}}[\text{Nb}_{13\text{nm}}/\text{Cu}_{27\text{nm}}]_{10}$ in applied field $\mu_0 H = 0.4$ T at temperatures (from left to right) $2.160 \text{ K} > T > 1.780 \text{ K}$, separated $\sim 5\text{-}15$ mK.. Horizontal dotted line delimit the experimental window used for scaling. (b) Derivatives of the $\log(I)$ - $\log(V)$ isotherms at temperatures (from bottom to top) $2.160 \text{ K} > T > 1.856 \text{ K}$. Black dots are within the experimental window used for scaling. The arrow marks derivatives of the isotherm at the lowest temperature showing decreasing slope in the low current limit